I. Appendix

A. Navigation coefficients

R_{app}, R_w, R_b, R_{tr} and R_a are formulated by appendix. equation (1).

$$\begin{cases} R_{app} = 0.5\rho S_A C_f (1+k_2) U^2 \\ R_w = c_1 c_2 c_5 \bigtriangledown e^{(m_1 F_r^d + m_2 cos(\lambda F_r^{-2}))} \\ R_b = 0.11 e^{-3P_B^{-2}} F_{ni}^3 A_{BT}^{1.5} \rho \dfrac{g}{1+F_{ni}^2} \\ R_{tr} = 0.5\rho A_T c_6 U^2 \\ R_a = 0.5\rho S_A C_A U^2 \end{cases} \tag{1}$$

where J is the advance speed ratio.

Appendix. Table I: Ship parameters

Description	Parameter	Full-scale	Scaling
Ship length	L_{pp}	230m	7.2785m
Ship breadth	B	32.2m	1.019m
Ship height	D	19m	0.6013m
Ship draft	T	10.8m	0.3418m
Block coefficient	C_b	0.651	0.651
Nomial Froude number	F_r	0.26	0.26
Nomial navigation speed	U	24.6 kn	2.196 m/s
Displacement	–	52030 ton	1.6489

B. Hybrid constraints

The SOC constraint is formulated by Appendix. equation (2).

$$\begin{cases} I_{min}^{char,SOC}(k) = \dfrac{SOC_{bat}(k) - SOC_{bat}^{max}}{\eta_i \triangle T / C_{bat}(k)} \\ I_{min}^{dis,SOC}(k) = \dfrac{SOC_{bat}(k) - SOC_{bat}^{min}}{\eta_i \triangle T / C_{bat}(k)} \end{cases} \tag{2}$$

where, $I_{min}^{char,SOC}$ and $I_{min}^{dis,SOC}$ are the minimum and maximum current range of battery based on SOC constraint, respectively; SOC_{bat}^{max} and SOC_{bat}^{min} are the maximum and minimum SOC ranges of battery, respectively.

In the voltage constraint, the voltage boundary to prevent the battery terminal voltage from exceeding the safe voltage range, i.e., the minimum voltage U_{bat}^{min} and the maximum voltage U_{bat}^{max} of battery, shown in Appendix. equation (3).

$$\begin{cases} U_{bat}^{min}(k) = OCV(k) - U_p(k) - R_0(k) I_{max}^{dis,vol}(k) \\ U_{bat}^{max}(k) = OCV(k) - U_p(k) - R_0(k) I_{min}^{char,vol}(k) \\ \quad OCV(k) = [OCV - \dfrac{\eta_i \triangle T}{C_{bat}} \dfrac{\partial OCV}{\partial SOC_{bat}} I_{bat}]|_{k-1} \end{cases} \tag{3}$$

where, $I_{min}^{char,vol}$ and $I_{max}^{dis,vol}$ are the minimum pulse current and the maximum pulse current caused by the voltage boundary, shown in Appendix. equation (4).

$$\begin{cases} I_{min}^{char,vol}(k) = \dfrac{OCV - U_p e^{-\Delta t/\tau} - U_{bat,max}}{\frac{\eta_i \Delta t}{C_{bat}} \frac{\partial OCV}{\partial SOC_{bat}} + R_p(1-e^{-\Delta t/\tau}) + R_0}|_k \\ I_{max}^{dis,vol}(k) = \dfrac{OCV - U_p e^{-\Delta t/\tau} - U_{bat,min}}{\frac{\eta_i \Delta t}{C_{bat}} \frac{\partial OCV}{\partial SOC_{bat}} + R_p(1-e^{-\Delta t/\tau}) + R_0}|_k \end{cases} \tag{4}$$

C. Solution process

Firstly, the equation (24) in the paper can be transformed into an optimal tracking control problem, as shown in equation (5).

$$\begin{aligned} minJ(I_{bat}^{ref}, I_{uc}^{ref}) = \sum_{k=1}^{N} \lambda_1 \| g(k) - h(k) \|^2 \\ + \lambda_2 \| i_{ILC}(k+1) - i_{ILC}(k) \|^2 \end{aligned} \tag{5}$$

where, h and g are the given value and the real value of ESS output, respectively; λ_1 and λ_2 are the weight coefficients.

The extreme value of the objective function can obtain the optimal solution: $i_{ILC}(k+1) = i_{ILC} + K_{N-1}[g(k) - h(k)]$. At this point, the iteration relationship of error is as: $[g(k) - h(k)] = L_N[g(k) - h(k)]$; where, K_{N-1} and L_N are the optimal gain matrix and the gradient, they all decrease as N increases.

According to the Karush-Kun-Tucker (KKT) conditions, if the control signal of HESS $u^* = [I_{bat}^{ref}, I_{uc}^{ref}]$ is the minimum, then we can get,

$$\begin{cases} \bigtriangledown J(u^*) + \sum\limits_{k}^{N} \lambda_j^* \bigtriangledown g_j(u^*) = 0, \\ \lambda_j^* \geq 0 \\ \lambda_j^* = 0, j \notin H(u^*) \end{cases} \tag{6}$$

In this mode, the equation (5) can be written in the following compact form:

$$\begin{cases} min(\dfrac{1}{2}\lambda^T H \lambda + \lambda^T P + \dfrac{1}{2}\gamma^T E^{-1} \gamma) \\ H = M E^{-1} M^T \\ P = \gamma + M E^{-1} F \\ u^* = -E^{-1}(F + M^T \lambda^*) \end{cases} \tag{7}$$

Then, the inequality constrained problem can be transferred to the equality constrained problem to improve the computing efficiency, as follows:

$$\lambda^* = -(M_{act} E^{-1} M^T)^{-1} (\gamma_{act} + M_{act} E^{-1} F) \geq 0 \tag{8}$$

where, M_{act} and γ_{act} are the relative matrix of active constraints. Finally, the quadratic programming procedure method can be used to find the optimal solutions.

In the stability analysis of hybrid control system, the transfer function of the learning algorithm is given as:

$$G_{ILC}(s) = K_{ILC} \frac{1}{1 + T_c s} \tag{9}$$

where, K_{ILC} and T_c are the gain of the ILC controller and time constant, respectively. When the control interval is $\Delta T = 5e^{-5}s$ with $e = 10$. The proposed control loop $|G_{ILC}(z) CR(z) G_I(z)|$ in the battery and the ultracapacitor are formulated by Appendix. equation (10) and Appendix. equation (11), respectively.

$$\begin{cases} K_{ILC}^{buck}\dfrac{1.223e^{-4}z^2-2.687e^{-6}z-1.196e^{-4}}{z^3-2.935z^2+2.87z-0.9355}, \text{Buck mode} \\ K_{ILC}^{boost}\dfrac{1.23e^{-4}z^2-1.334e^{-6}z-1.204e^{-4}}{z^3-2.947z^2+2.894z-0.9474}, \text{Boost mode} \end{cases} \tag{10}$$

$$\begin{cases} K_{ILC}^{buck}\dfrac{1.223e^{-4}z^2-2.687e^{-6}z-1.196e^{-4}}{z^3-2.935z^2+2.87z-0.9355}, \text{Buck mode} \\ K_{ILC}^{boost}\dfrac{1.23e^{-4}z^2-1.326e^{-6}z-1.204e^{-4}}{z^3-2.947z^2+2.895z-0.9474}, \text{Boost mode} \end{cases} \tag{11}$$

Therefore, the locus of the hybrid control system cannot exceed the unit cycle, and the associated Nyquist diagram of the battery and the ultracapacitor are shown in Appendix. Fig. 1, respectively. To ensure the stability of the system and achieve the fast convergence of the system, the gain K_{ILC}^{buck} and K_{ILC}^{boost} of the battery are chosen as 2 and 0.6 by experimentation in buck mode and boost mode, respectively; the gain K_{ILC}^{buck} and K_{ILC}^{boost} of the ultracapacitor are chosen as 3 and 0.5 in buck mode and boost mode, respectively.

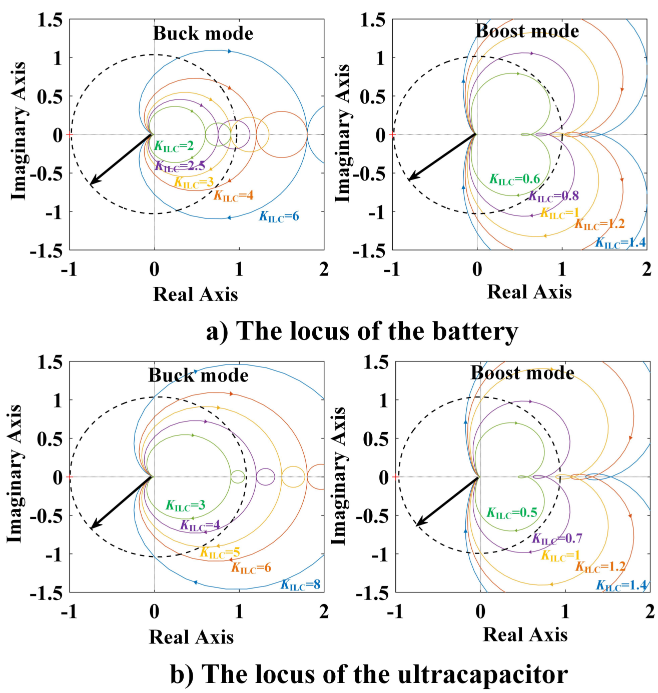

Appendix. Fig. 1. The locus of $G_{ILC}(z)CR(z)G_I(z)$ of the HESS.